CONF-810902--1

LA-UR -81-909

TITLE: PERFORMANCE PREDICTIONS AND MEASUREMENTS FOR SPACE-POWER-SYSTEM HEAT PIPES

MASTER

AUTHOR(S): F. COYNE PRENGER, JR.

SUBMITTED TO: FOURTH INTERNATIONAL HEAT PIPE CONFERENCE
LONDON, ENGLAND
SEPTEMBER 7-10, 1981

University of California

LOS ALAMOS SCIENTIFIC LABORATORY
Post Office Box 1663 Los Alamos, New Mexico 87545
An Affirmative Action/Equal Opportunity Employer

Form No. 836 R3
St. No. 2629
12/78

UNITED STATES
DEPARTMENT OF ENERGY
CONTRACT W-7405-ENG. 36

PERFORMANCE PREDICTIONS AND MEASUREMENTS FOR SPACE-POWER-SYSTEM HEAT PIPES

F. Coyne Prenger, Jr.*

*Staff Member, Los Alamos National Laboratory
Los Alamos, New Mexico 87545

ABSTRACT

High temperature liquid metal heat pipes designed for space power systems have been analyzed and tested. Three wick designs are discussed and a design rationale for the heat pipe is provided. Test results on a molybdenum, annular wick heat pipe are presented. Performance limitations due to boiling and capillary limits are presented. There is evidence that the vapor flow in the adiabatic section is turbulent and that the transition Reynolds number is 4000.

INTRODUCTION

Proposed future space missions require large quantities of electrical power for space-based remote sensors and spacecraft propulsion. Numerous Earth-orbit missions involving surveillance and communications have been defined.[1] Transportation to geosynchronous orbit can be done efficiently with nuclear electric propulsion systems if transit times of one year are acceptable. In addition, these power systems extend the capability to investigate the outer planets and to perform solar escape missions.

Although several system designs have been studied,[2] certain features appear to be common to all designs. For the heat source, a reactor containing refractory nuclear fuel, which will allow source temperatures as high as 1700 K, is favored. Gas-cooled and liquid-cooled configurations have been considered, but a heat-pipe-cooled design offers high reliability, redundancy, and minimum weight. Heat pipes are used to transfer heat from the reactor core to the power converters. Both passive and dynamic converters have been considered. Despite their low efficiencies, the passive converters, i.e., thermoelectrics and thermionics, represent the lowest specific weight systems.[2] In all of the proposed systems, however, reliable heat transport with small temperature drops between the reactor and converters is required. High temperature (1400-1700 K) liquid metal heat pipes are being developed and tested at the Los Alamos National Laboratory for use in nuclear electric power applications in space.

Both stainless steel and molybdenum heat pipes with composite wick structures have been analyzed. Working fluids include both sodium and lithium. The wick structures considered include a porous screen, screen-covered grooves, and

circular arteries. Performance limits for these heat pipes have been calculated and they include the effects of bends and the influence of long adiabatic zones.

Test data have been obtained on both molybdenum and stainless steel heat pipes using sodium as the working fluid. Sonic, wicking, and boiling limits have been observed. These data have been compared with analytical predictions and the results provide empirical data on pressure drop and transition flow in the adiabatic zones of these heat pipes.

ANALYSIS

Wick Design

Three wick designs were evaluated in the heat pipe development program. The three designs are shown in Fig. 1 and include screen-covered axial grooves, a porous tube insert forming an eccentric annular gap and circular arteries. The screen-covered axial groove design was considered first primarily because grooved stainless steel tubing was readily available and the method of installation of the screen cover was proven. It was recognized, however, that the artery design, although more difficult to fabricate, offered superior performance. A comparison between the artery and grooved-wick design, assuming laminar flow, is shown in Fig. 2. At the design operating temperature of 1400 K the artery configuration shows significantly better performance. However, the reactor design requires bends in the heat pipe adiabatic section and since preliminary bending tests were successfully performed on a grooved-wall heat pipe, a test program was initiated using a screen-covered groove wick design.

During the first experiments with this wick structure, heat transfer limits well below those calculated were measured. Based on some earlier work with carbon contaminated heat pipes, it was suspected that this impurity, introduced by a lubricant during groove fabrication, was collecting in the evaporator and reducing the liquid surface tension. This problem was somewhat alleviated by cold trapping, a standard procedure for reducing the content of carbon and other impurities from sodium. Results of the tests on stainless-steel, screen-covered, groove heat pipes have been reported.[3] Analysis showed that a screen pore size of 35 μm was required to achieve 20 kW at 1400 K. Although a 35 μm pore size has been achieved with stainless steel screens, such a small pore size may not be possible using molybdenum which will ultimately be required in the final design. Therefore, the screen-covered groove design was abandoned in favor of an annular wick design.

It was necessary to initiate a test program to evaluate the effect of long adiabatic sections and bends on heat pipe performance. The simplest heat pipe internal configuration to study the performance limitations of long adiabatic sections, and one that was amenable to bending, was an annular-gap wick design. Analysis showed that the performance of an annular wick design approaches that of the artery design; therefore, an annular wick heat pipe was fabricated for performance evaluation and the results are presented in the following section. However, since this design uses a porous tube that is inserted into the heat pipe to create the liquid return passage, there is only a single liquid flow path. Therefore, any condition that results in either the generation of a vapor bubble or the introduction of an impurity gas at the heat pipe wall will lead to evaporator dryout and heat pipe failure. Also, the annular gap design requires that the heat be transferred through the liquid layer adjacent to the heat pipe wall. This leads to significant radial temperature gradients within the heat pipe.

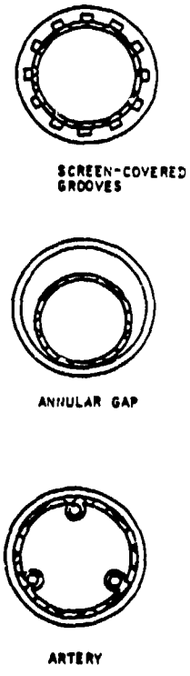

Fig. 1. Heat pipe internal geometries.

Because of these limitations, an artery design for the core heat pipes was investigated. By having multiple arteries, redundant liquid flow passages are provided. Also, by collecting the liquid in discrete locations around the circumference of the heat pipe, large temperature drops across the liquid layer are avoided. Figure 3 shows a performance map of a two-artery heat pipe as a function of temperature and screen thickness. The screen thickness for both the arteries and the distribution wick are optimum at 0.3 mm (0.012 in.). If the screen thickness is too large, the vapor flow area is reduced excessively; whereas, if the screen is too thin, the circumferential pressure drop in the distribution wick increases. Consideration of these two effects dictates an optimum screen thickness.

Development of a successful wick design for the core heat pipes has been an evolutionary process. The process started with the screen-covered grooves which represented a known technology and progressed to an annular wick design which was used to obtain needed test data on the effects of long adiabatic sections and bends. Finally, boiling limitations and lack of redundancy have indicated an artery design to be more feasible. Subsequent tests will show if the artery design is adequate.

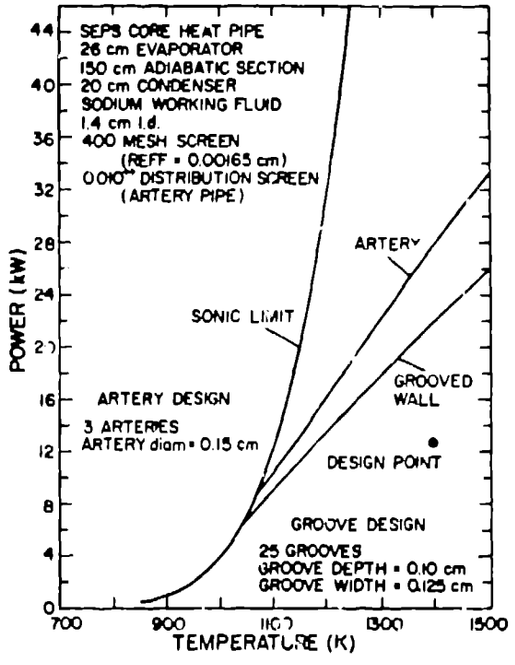

Fig. 2. Performance curves for SPAR core heat pipes.

Working Fluid

Sodium and lithium were considered as working fluids for the core heat pipe application. A comparison of the two working fluids is shown in Fig. 4. Lithium has both a higher surface tension and a higher latent heat of vaporization than sodium. In addition, the reaction rates in the oxygen-molybdenum system appear to be much slower with lithium compared to sodium. These are important considerations and give lithium a distinct advantage over sodium. However, at 1400 K the sonic limit of lithium is lower than the design power of 12.5 KW. This is the principal reason why sodium was selected as the working fluid for this application. A significant performance penalty is paid if the heat pipe is operated near the sonic limit. High vapor velocities are encountered with accompanying higher pressure and temperature drops. This causes operation at a lower converter temperature reducing system efficiency and increasing system weight.

Pore Size

The effect of pore size for both the screen tube and artery design is shown in Fig. 5. These results indicate a larger liquid pressure drop in the screen tube compared with an artery design employing three arteries. In fact, the liquid pressure drop in the artery design is so low that no significant decrease in performance occurs with the loss of one artery. The effect of circumferential

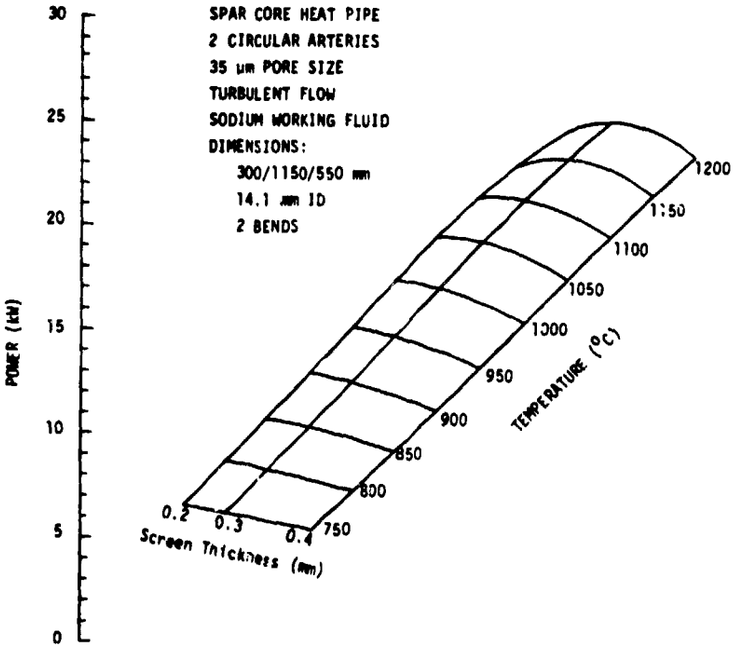

Fig. 3. Performance map of two-artery heat pipe for SPAR.

pressure drop on the heat p pe performance is not included in the results of Fig. 5. As mentioned earlier, as the pore size decreases the flow resistance of the screen increases. This increase creates a higher circumferential pressure drop in the artery heat pipe. Ways to overcome this have been proposed such as using a different screen with a different pore structure for the distribution wick. A local failure in the surface film in the artery wall results in complete failure of the artery; whereas, a local failure in the surface film in the distribution wick creates only a local dry-out, and cooling of the adjacent wall areas renders this condition less serious.

Although the design power is achieved with a pore size of 50 µm, a pore size of 35 µm is the design goal giving a performance margin of two. Small pore sizes have been obtained with 150 mesh molybdenum screen by drawing and swaging of multiple layers. In the next section test results obtained with a molybdenum annular-wick heat pipe are presented.

Experiments

SPAP-1, a 2-m-long molybdenum heat pipe, was assembled with a recrystallized, low-carbon, arc-cast molybdenum container tube that was 2 m long by 15.9 mm o.d. with a 0.94-mm-thick wall. A molybdenum collar was joined to the tube by electron beam welding at the beginning of the condenser section of the heat pipe. A calorimeter was bolted to the welded collar and isolated from the condenser

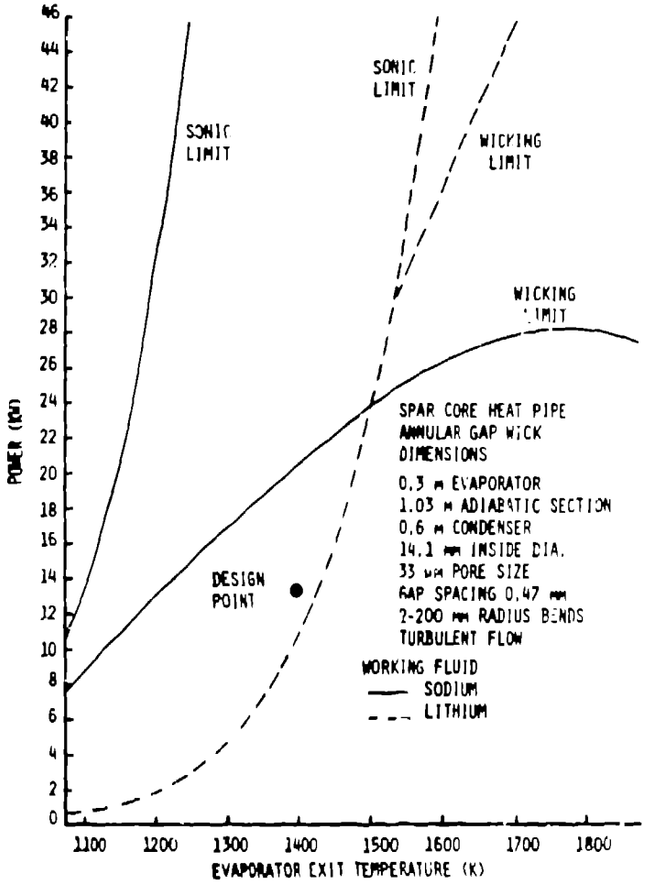

Fig. 4. Comparison of sodium and lithium working fluids.

section of the heat pipe during testing. Both end caps and fill tube were joined to the tube by electron beam welding, and a copper-brazed, stainless-steel Swagelok fitting and a stainless steel extension were attached to the recrystallized, low-carbon, arc-cast molybdenum fill tube. The outside diameter of the screen tube was 12.8 mm and it had a wall thickness of 0.23 mm. The screen tube, which was plugged at one end with a tapered molybdenum plug, was 1.984 m long and fit into the container tube. A 0.61-mm radial gap existed between the container tube and the screen tube. The screen tube was installed, plugged end first, into the container tube after the blind end cap had been welded on and after a 8.5 g stack of hafnium foil had been inserted. The fill end cap with its attached fill tube, brazed Swagelok fitting, and stainless steel extension tube was electron beam welded to the container tube completing the assembly.

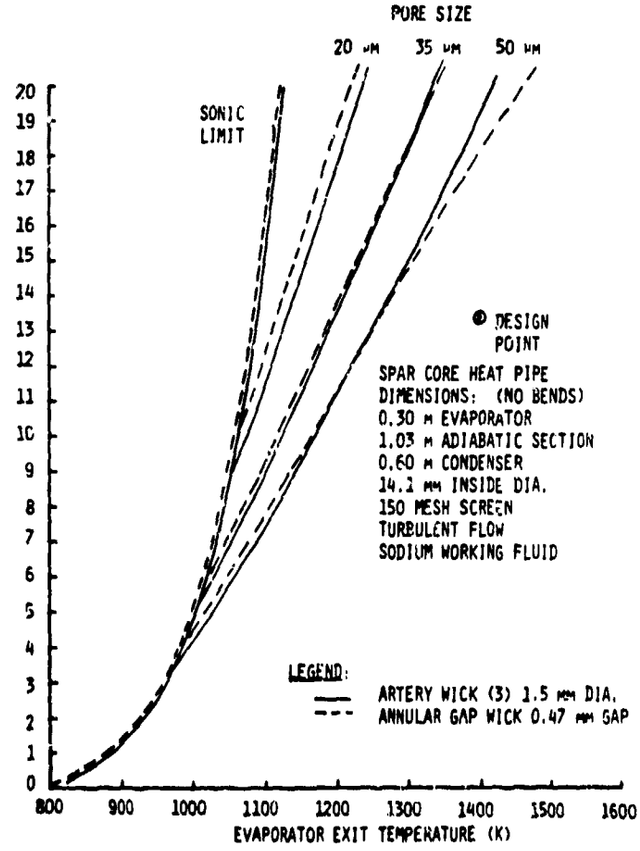

Fig. 5. Effect of pore size on heat pipe performance.

Sodium was vapor distilled into the heat pipe as the working fluid. After the annular liquid flow passage was filled, a sodium pool of 320 mm remained at one end. Since this heat pipe will be operated with a negative 5 deg tilt (evaporator up), the liquid pool will be at the end of the condenser and will reduce the effective condenser length to 330 mm. The evaporator length is 300 mm and is shifted 50 mm from the end of the heat pipe leaving a 1.0-m adiabatic section. The heat pipe is shown schematically in Fig. 6.

Preliminary testing of the heat pipe without the calorimeter attached was conducted. The heat pipe was operated horizontally at 1400 K. To evaluate the degree of wetting by the working fluid, the condition of the porous tube, and the amount, if any, of noncondensible gas in the heat pipe, the test procedure was to increase the tilt of the heat pipe (evaporator up) during operation until

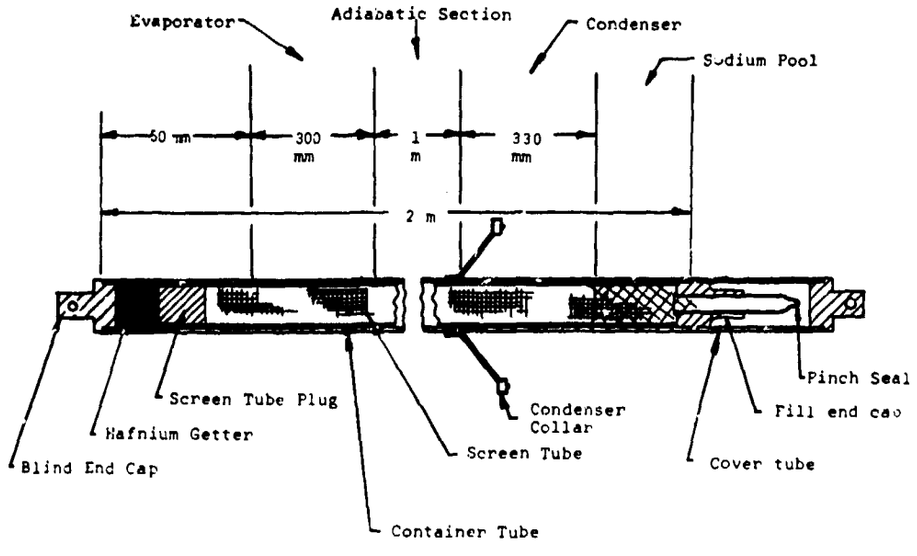

Fig. 6. SPAR-1 heat pipe.

a dryout was encountered. By knowing the maximum tilt angle and the heat load, an effective pore size for the porous tube can be obtained using the heat pipe computer code HTPIPE.[4] The maximum tilt angle was 55 deg and the heat pipe operating temperature was 1200 K. For a heat load of 785 W, the pore size was 47 μm.

Results

A comparison between the data obtained from the SPAR-1 tests and the results of the performance analysis from the heat pipe computer code was made. Figure 7 shows the performance limits obtained from the tests along with the predicted wicking, sonic, and boiling limits for both laminar and turbulent vapor flow. The predicted wicking limits are based on a wick pore size of 47 μm as determined from the no-load tilt test of the heat pipe.

The decrease in measured performance at temperatures above 1250 K is indicative of boiling at the heat pipe wall. The resulting vapor formation in the liquid return passage causes evaporator dryout. Curve 5 in Fig. 7 represents the boiling limit as a function of temperature and is based on the experimental data. Since SPAR-1 contains an unsupported screen wick, the liquid layer is thicker on one side of the wick. By centering the screen wick, the maximum liquid layer thickness can be reduced and the boiling limit raised. For the same size nucleation site, Curve 6 of Fig. 7 shows the boiling limit for the centered wick configuration. This results in a significant increase in the boiling limit.

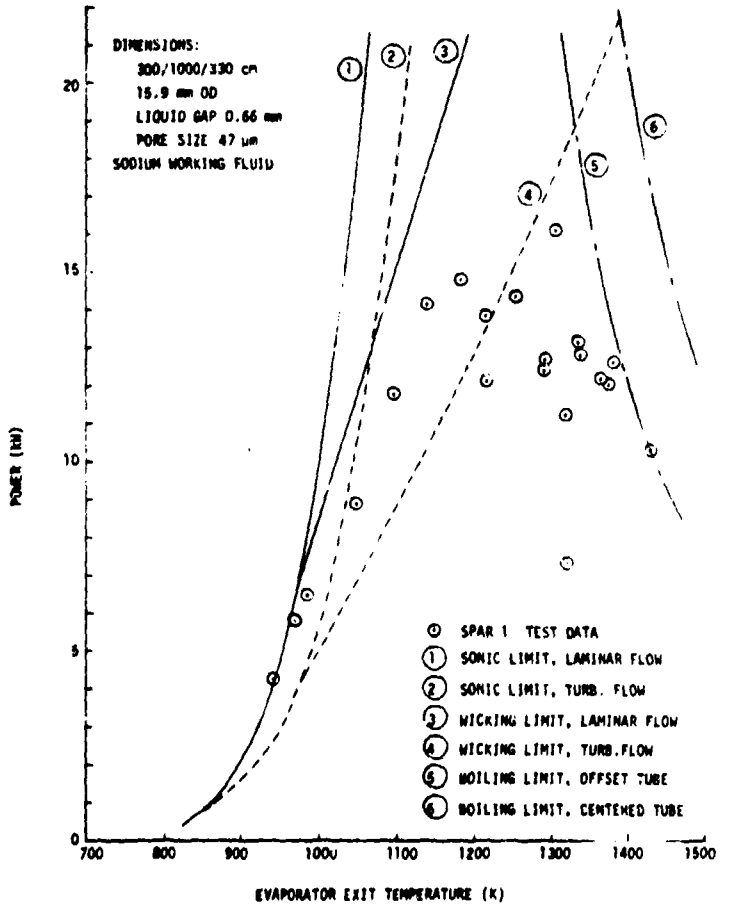

Fig. 7. Comparison between analysis and test for SPAR 1.

The wicking limits measured at temperatures below 1250 K lie between the laminar and turbulent vapor flow predictions as shown in Fig. 8. Agreement between the model and the data is achieved if a transition Reynolds number in the adiabatic section of 4000 is assumed. This corresponds to a friction factor of 0.004 which lies between the laminar and turbulent value. This result is also shown in Fig. 8. It is likely that the vapor flow in the evaporator section is laminar because of the stabilizing effect of the mass addition to the vapor stream. At some point in the adiabatic section the effects of friction and inertia cause the flow to become turbulent. Other factors may influence this result especially the presence of bends in the adiabatic section. Figure 9 shows the Fanning friction factor as a function of Reynolds number for a transition Reynolds number of 4000. It should be noted that the friction factor corresponding to Re = 4000 is 0.004 and remains constant with increasing Reynolds number until the turbulent friction factor calculated from Blasius' equation becomes less than 0.004, at which time the Blasius result is used.

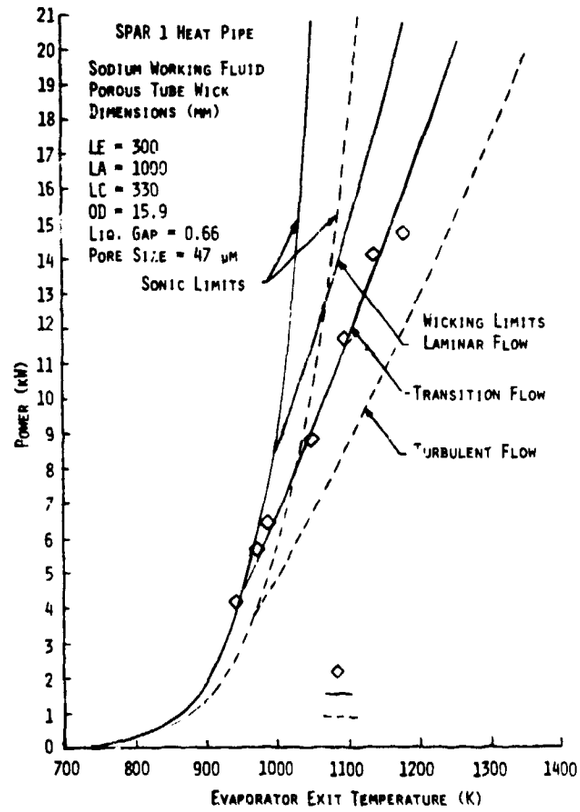

Fig. 8. SPAR 1 wicking limits with 47 μm pore size.

The sensitivity of the heat pipe performance to friction factor is significant as shown by Fig. 8 but, unfortunately, can only be determined empirically at the present time. Further tests, especially with heat pipes containing bends, may provide information that can be used to predict transition Reynolds numbers for alternative configurations.

DISCUSSION

Boiling Limit

Testing of the SPAR-1 heat pipe has indicated performance limitations based on the formation of vapor bubbles in the annular liquid passage. The mechanism for producing these vapor bubbles is dependent on the number and size of nucleation sites on the heat pipe wall and on the local heat flux that determines the amount

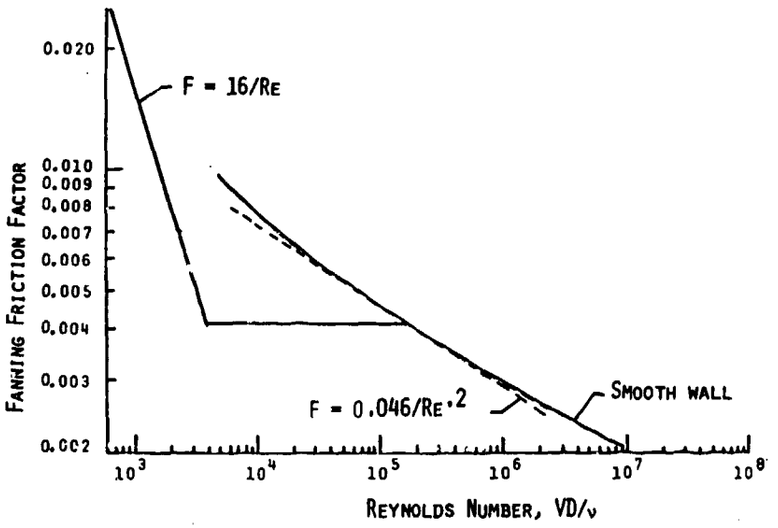

Fig. 9. Friction factor for SPAR-1 heat pipe.

of superheat available for bubble growth. Whether or not the vapor bubble that forms on the heat pipe wall will grow depends on a force balance across the vapor-liquid interface. For a bubble in equilibrium the pressure difference across the interface is balanced by the liquid surface tension or

$$P_v - P_l = \frac{2\sigma}{R}, \tag{1}$$

where

P_v is the vapor pressure corresponding to the heat pipe wall temperature;
P_l is the liquid pressure in the annulus;
σ is the liquid surface tension; and
R is the bubble radius.

The configuration is illustrated in Fig. 10.

To calculate the radius of the nucleation site, the vapor pressure within the bubble must be determined. Assuming that the bubble is small relative to the thickness of the liquid layer, the vapor pressure within the bubble corresponds to the heat pipe wall temperature which is a function of the local heat flux and the thermal conductivity of the liquid. For a circular heat pipe, the temperature drop across the liquid layer is given by:

$$T_w - T_v = \frac{q \ln\left(r_w/r_r\right)}{2\pi LK}, \tag{2}$$

where

T_w is the heat pipe wall temperature;
T_v is the vapor temperature;

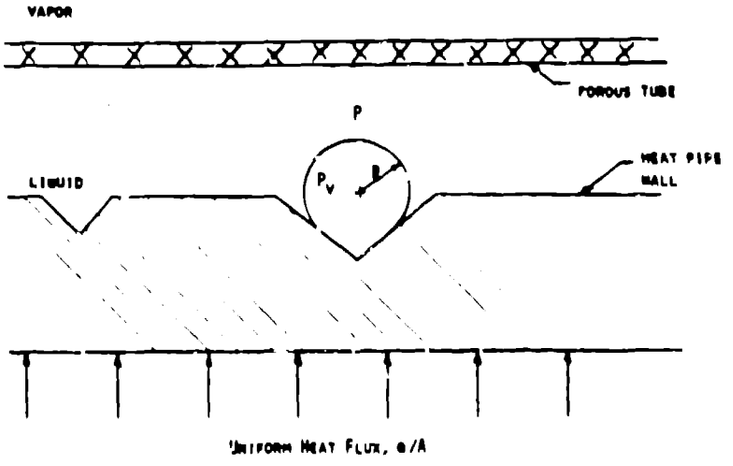

Fig. 10. Vapor bubble formation at the heat pipe wall.

q is the heat transfer;
r_w is the inside radius of the heat pipe wall;
r_r is the inside radius of the heat pipe wick, distribution screen, or porous tube;
L is the length of the heat pipe evaporator; and
K is the liquid thermal conductivity.

Equation (2) is used to find the wall temperature, and the corresponding vapor pressure is then determined. Using Eq. (1) the equilibrium vapor bubble radius can then be found.

Figure 11 shows the pore radius as a function of heat pipe power for both the artery and the annular gap wick design. For each value of the heat pipe power there corresponds an evaporator exit temperature specified by the wicking limit. This was the heat pipe temperature assumed in calculating the vapor bubble size. The pore radius given in Fig. 11 is the maximum radius of a nucleation site that can be tolerated for the given power and temperature. Any nucleation site, created by incomplete wetting of a surface imperfection, which exceeds this radius will generate an unstable vapor bubble, i.e., the bubble will grow and ultimately form a vapor pocket in the liquid passage. This vapor pocket will bridge the liquid passage causing a dryout to occur.

In the artery design the liquid is collected in arteries which are isolated from the heat pipe wall by a distribution screen. The distribution screen is thin compared with the liquid layer in the annular gap, and a larger nucleation site can be tolerated at the same power level in the artery design. This is shown in Fig. 11. The reduced superheat together with the ability to tolerate localized hot spots makes the artery design superior.

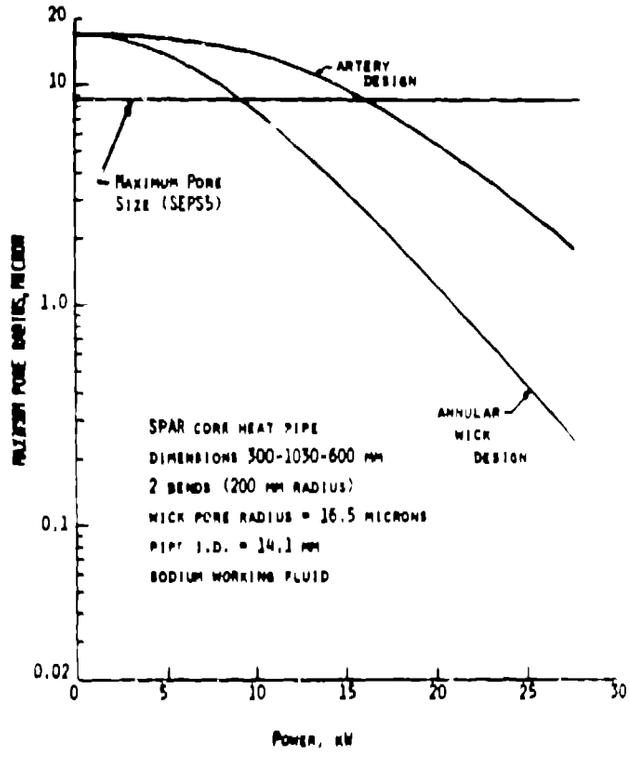

Fig. 11. Maximum size nucleation site.

Optimum Wick Design

Experience has been gained with three heat pipe wick designs although testing of the artery design has not been accomplished. During testing, poor performance due to impurities was experienced with the grooved-wall configuration. Also, potential superheat problems due to the relatively thick heat pipe wall contributed to development of the annular wick and artery designs subsequently pursued. Performance limits for the annular wick and artery designs are similar. A comparison between the two designs is shown in Table I. Only two significant drawbacks exist for the artery design; difficulty of fabrication especially if bending of the heat pipe is required and filling uncertainties associated with amount of working fluid and proper filling of the arteries. Whereas, the annular wick design suffers from excessive superheat, which lowers the boiling limit, and no redundancy in the liquid flow passage.

A continuing experimental test program is required to better understand the vapor pressure drop limitations in high-performance heat pipes containing bends and long adiabatic sections. Preliminary test results have indicated that a transition to turbulent flow of the vapor occurs in the adiabatic section. Further, this transition occurs at Reynolds numbers based on tube diameter of approximately 4000. What effect bends will have on thir transition is of paramount interest.

TABLE 1 Comparison Between Artery Wick Design and Annular Wick Design

	Annular Wick	Artery Wick
Advantages	• Ease of fabrication and assembly	• Redundant liquid passages
	• No circumferential distribution of working fluid required	• Impurities collect in distribution wick causing only local hot spots
	• Simple geometry enabling accurate calculation of liquid invertory	• More tolerant of wick damage
Disadvantages	• Sensitive to boiling limits	• Difficulties in assembly (intimate contact with wall required)
	• No redundant liquid passages	• Provide excess working fluid to fill artery (fillets require excess working fluid)
	• Collection of impurities in evaporator may result in single point failure	

REFERENCES

1. Buden, D. (1979). Missions and Planning for Nuclear Space Power, 14th Intersociety Energy Conversion Engineering Conference. Boston, MA.
2. Buden, D. (1979). Selection of Power Plant Elements for Future Reactor Space Electric Power Systems, 14th Intersociety Energy Conversion Engineering Conference, Boston, MA.
3. Prenger, F. C., and Kemme, J. E. (1979). Performance Limits of Liquid Metal Heat Pipes Containing Long Adiabatic Sections, 14th Intersociety Energy Conversion Engineering Conference, Boston, MA.
4. Prenger, F. C. (1979) Heat Pipe Computer Program (HTPIPE) User's Manual, Los Alamos National Laboratory report LA-8101-M.